Articles in PresS. J Appl Physiol (August 20, 2009). doi:10.1152/japplphysiol.91322.2008

Dynamic Correction for Parallel Conductance, G_P, and Gain Factor, α, in Invasive Murine Left Ventricular Volume Measurements

JOHN E. PORTERFIELD[1], ANIL T.G. KOTTAM[2], KARTHIK RAGHAVAN[1], DANIEL ESCOBEDO[3], JAMES T. JENKINS[3,4], ERIK R. LARSON[1], RODOLFO J. TREVIÑO[3], JONATHAN W. VALVANO[1], JOHN A. PEARCE[1], AND MARC D. FELDMAN[2,3,4]

[1] Department of Electrical and Computer Engineering, The University of Texas, Austin, TX
[2] Department of Biomedical Engineering, The University of Texas, Austin, TX
[3] Division of Cardiology, The University of Texas Health Science Center, San Antonio, TX, and
[4]The South Texas Veterans Health Care System, San Antonio, TX

Running Head: Dynamic G_P and α Correction

Correspondence:

Marc D. Feldman, MD
University of Texas HSC
Room 5.642 U
7703 Floyd Curl Drive
San Antonio, TX
78229-3900
Ph: 210-567-2106
Fax: 210-567-6960
E-mail: feldmanm@uthscsa.edu

Abstract - The conductance catheter technique could be improved by determining instantaneous parallel conductance (G_P) which is known to be time-varying, and by including a time-varying calibration factor in Baan's equation ($\alpha(t)$). We have recently proposed solutions to the problems of both time-varying G_P and time-varying α, which we term "admittance" and "Wei's equation", respectively. We validate both our solutions in mice, compared to the currently accepted methods, hypertonic saline (HS) to determine G_P and Baan's equation calibrated with both stroke volume (SV) and cuvette. We performed simultaneous echocardiography in closed chest mice (n=8) as a reference for left ventricular (LV) volume, and demonstrate that an off-center position for the miniaturized Pressure-Volume (PV) catheter in the LV generates end-systolic and diastolic volumes calculated by admittance with less error ($p<0.03$) (-2.49±15.33 µl error) compared to those same parameters calculated by SV calibrated conductance (35.89±73.22 µl error), and by cuvette calibrated conductance (-7.53±16.23 µl ES and -29.10±31.53 µl ED error). To utilize the admittance approach, myocardial permittivity (ε_m) and conductivity (σ_m) were calculated in additional mice (n=7) and those results are used in this calculation. In aortic banded mice (n=6) increased myocardial permittivity was measured (11844±2700 control, 21267±8005 banded, $p<0.05$), demonstrating that muscle properties vary with disease state. Volume error calculated with respect to echo did not significantly change in aortic banded mice (6.74±13.06 µl, p=NS). Increased inotropy in response to iv dobutamine was detected with greater sensitivity with the admittance technique compared to traditional conductance (4.9±1.4 to 12.5±6.6 $mmHg \cdot \mu l^{-1}$ Wei's equation ($p<0.05$), 3.3±1.2 to 8.8±5.1 $mmHg \cdot \mu l^{-1}$ using Baan's equation (p=NS). New theory and method for instantaneous G_P removal, as well as application of Wei's equation, are presented and validated *in vivo* in mice. We conclude that for closed-chest mice, admittance (dynamic G_P) and Wei's equation (dynamic α) provide more accurate volumes than traditional conductance, are more sensitive to inotropic changes, eliminate the need for hypertonic saline, and can be accurately extended to aortic banded mice.

Keywords - Conductance catheter, parallel conductance, mouse, left ventricular, admittance, α, pressure volume relationship

I. Introduction

The conductance technique was first proposed by Baan 28 years ago to provide an invasive instantaneous left ventricular volume signal to generate left ventricular pressure-volume relations and hemodynamic indices from the pressure – volume plane [1]. The original theory as proposed relates conductance to volume through a simple equation based on stroke volume, resistivity of blood, and the length between the voltage contacts of the catheter, L:

$$Volume = \frac{\rho L^2}{\alpha}\left(G - G_P\right), \tag{1}$$

where ρ represents the resistivity of blood (Ω-m), L represents the length between the voltage contacts (m), α is a constant gain factor dependent on the stroke volume (Baan assumed it to be a constant α = 1, implying a uniform current field distribution), G is the total conductance measured (S), and G_P is the muscle conductance in parallel (S) and assumed to be constant.

There are two major criticisms of this method. The first is that α, the calibration factor in Baan's equation, is not a constant but instead changes dynamically as the moving heart wall changes the shape of the applied electric field [29]. The second is that as the LV contracts and fills, the cardiac muscle moves closer to and farther away from the catheter, so subtracting a constant as in Equation 1 probably does not adequately compensate for the parallel muscle conductance [29]. The latter problem is exacerbated by the aortic valve being off center relative to the midline of the LV chamber in mammalian hearts. This forces the miniaturized PV catheter to be closer to the septum than the midline (Figure 1A, [23]). Additionally, preload reduction used to generate load independent measures of contractility is anticipated to further exacerbate any error from the

currently practiced constant measure of parallel conductance. Thus, there is a need for a dynamic measurement technique to quantify both G_P and α [29].

The conductance technique has historically been used in large animals and humans. More recently, in 1998, the technique was extended to the murine heart to characterize gene-altered mouse models [11, 23]. Due to the small size of the mouse heart, newer α calibration methods have been developed. For example, cuvettes of known volume are used to determine a linear conductance to volume relationship that is often used as the primary calibration method [3, 5, 13, 22, 32]. Additionally, α can be calculated as a constant ratio of conductance stroke volume to a known standard for stroke volume (usually an aortic flow probe or echo) [4, 9, 15, 16, 19, 25, 27]. Most of these publications also use the hypertonic saline method to determine the parallel conductance value (G_P) as a constant. However, the historical sources of error outlined above still exist in these studies. There is a need for newer solutions to solve these two long standing sources of error.

We have recently proposed solutions to both dynamically changing parallel conductance G_p [29] and dynamically changing α [30] that we term "admittance" and "Wei's equation", respectively. Neither solution has been compared to the currently accepted standards (i.e. cuvette calibrated or SV calibrated use of Baan's equation and hypertonic saline) to date either by ourselves or by others [21, 23]. By using echocardiography as the standard of comparison for true left ventricular volume, we now compare our proposed solutions with Baan's original technique in the intact murine heart.

Terminology:

Ohm's law: V = IR where V is voltage, I is current, and R resistance, alternatively I = VG where G is conductance.

Conductance, or G (μS), G_P (μS) Parallel Conductance, G_B Conductance of Blood (μS), and G_M Conductance of Muscle (μS)

Conductivity, or σ (μS/cm)

Resistivity, or ρ (Ω x m) = 1/conductivity

Admittance, or $\boldsymbol{Y} = \bar{Y}$ = I/V = G (real) + jB (imaginary), where

G = conductance, j = square root of -1, B = ωC. ω = 2πf (f = frequency), C = capacitance.

Magnitude $|\boldsymbol{Y}| = \sqrt{(G^2 + B^2)}$, and Phase angle $(\theta) = \tan^{-1}$ (B/G), where B and G are defined above.

Wei's Equation, conversion from conductance to volume that utilizes a variable α to describe the dynamic field shape.

Permittivity: $\varepsilon = \varepsilon_r \varepsilon_0$ (F/m). $\varepsilon_0 = 8.85 \times 10^{-12}$ (F/m)

Cell Constant k (m^{-1})

Field Geometry Factor $F = 1/k = G_{saline}/\sigma_{saline}$ (m)

II. Materials and Methods

Instrumentation Overview. Custom hardware has been developed by our group to produce a complex admittance signal (both magnitude and phase) compatible with any size tetrapolar conductance catheter. For the present study, we focused on murine sized hearts.

The block diagram of the entire system is shown in Figure 1 based on our previous design [7]. A 20 kHz voltage sine wave drives a voltage-to-current amplifier, which is used to produce the stimulation current for electrodes 1 and 4. Leads 2 and 3 are fed into an instrumentation amplifier (AD 624, Analog Devices, Norwood MA), which measures the potential difference created by the induced electric field in the blood pool. The signal is then filtered and rectified, and the inverse taken by a multiplier chip (AD 734, Analog Devices) in order to transform the impedance signal to an admittance signal. This output is taken as the magnitude of the admittance signal $|\boldsymbol{Y}|$.

We designed and developed a phase angle (θ) detection system using discrete analog components that determines the phase angle between two input sinusoidal signals, which is also shown in the block diagram in Figure 1. A simplified diagram to explain how phase (θ) is measured is shown in Figure 2. Figure 2 simplifies the measurement system to its most basic building blocks, the two electrodes, and a uniform field distribution (as is assumed by Baan's equation). The basis of the admittance technique relies on a measurable phase difference (θ) due to the presence of myocardium between the input current and the output voltage (Figure 2C), while there is no measurable phase angle in blood alone (Figure 2A and [24]). However, both muscle and blood have measurable electrical conductivity, which affects the output signal magnitude (the admittance magnitude is simply the ratio of input current to output voltage). The relative fraction of muscle and blood in the measurement determines the value of the admittance magnitude and phase angle (Figure 2B). Separation of myocardium and blood is possible during the measurement. Traditionally, the phase of the admittance has been overlooked as a source of information, and the admittance magnitude has been mistaken for the conductance. In

this study, the admittance technique defines the conductance as the real part of the complex admittance G = Real{$\boldsymbol{Y}$} = |$\boldsymbol{Y}$| · cos (θ), while the conductance technique defines it as G = |$\boldsymbol{Y}$| (only a correct assumption if there is no measurable phase angle).

Murine Studies. The Institutional Animal Care and Use Committees at the University of Texas Health Science Center at San Antonio and at the University of Texas at Austin approved all experiments. A total of 38 mice were studied. The background strain was C57BlkS/J, ages 3-11 months. Mice were placed on a heated, temperature controlled operating table for small animals (Vestavia Scientific, Birmingham Alabama). Experiments were performed at a murine body temperature of 37°C.

Admittance (Wei's equation) – Hypertonic Saline (Baan's equation) Comparison to Echo. Mice were anesthetized by administration of 1-2% Isoflurane and were allowed to breathe spontaneously with 100% supplemental O_2. The right carotid artery was entered and a tetrapolar micro-manometer catheter (Scisense, Inc., London, Ontario) was advanced into the LV of the intact beating mouse heart. The right jugular vein was cannulated for later administration of 10 μl of 3% hypertonic saline to determine steady state parallel conductance as previously described [6]. A total of n=8 mice were studied. The position of the tetrapolar catheter in the LV was guided by simultaneous imaging with a transthoracic echocardiogram (VisualSonics, Toronto, Canada). The initial position for placement of the tetrapolar catheter was the off-center location (see Figure 3B). In the off-center position, instantaneous LV PV relations were monitored to assure that a physiologic loop was obtained before acquiring data for both the admittance and conductance raw signals. Final acceptance of the catheter position was based upon both echocardiography and the appearance of the loop. Data acquisition consisted of simultaneous LV pressure, conductance (no phase) stimulated at 20 kHz, and complex admittance (magnitude and phase) also at 20 kHz, and echocardiographic images plus ECG for later calculation of end-diastolic volume (EDV), end-systolic volume (ESV), and stroke volume (SV). An operating frequency of 20 – 25 kHz maximizes the observable muscle signal [24]. All data were sampled at 1 kHz.

Subsequently, the tetrapolar catheter was re-positioned to be in the center of the left ventricular cavity (see Figure 3A), with final positioning confirmed by both echocardiography and a physiologic LV PV loop. Data acquisition for simultaneous LV pressure, conductance, admittance, and echocardiographic images plus ECG for later calculation of EDV, ESV, and SV were repeated. A 10 µl bolus of 3% hypertonic saline was administered n=3 times per mouse via the right jugular vein, for later determination of steady state parallel conductance, as previously described [6].

Admittance (Wei's equation) – Hypertonic Saline (Baan's equation) Comparison During IVC Occlusion. An additional group of mice (n=4) were studied. Mice were anesthetized by administration of 1-2% Isoflurane, intubated, and mechanically ventilated at 100% O_2 with a rodent ventilator set at 150 breaths/min. The heart was exposed via an anterior thoracotomy. An apical stab was made in the heart with a 30G needle, and the tetrapolar micro-manometer catheter was advanced retrograde into the LV along the long axis with the proximal electrode just within the myocardial wall of the apex. The inferior vena cava (IVC) was isolated immediately below the diaphragm for transient occlusion.

Baseline LV pressure-conductance loops and pressure-admittance loops were acquired. Data were subsequently acquired during transient occlusion of the IVC. A small animal blood flow meter (T106, Transonic Systems Inc., Ithaca, NY) was used with a 1.5mm Transonic flow probe (MA1.5PSL) placed on the ascending thoracic aorta and simultaneous LV conductance, admittance, pressure and aortic flow were recorded. The flow probe was used to determine the SV for calibration of the final volume signal in this study, instead of echo.

Dobutamine Studies. A study was performed in n=6 mice (C57BlkS/J, female, body weight 23±2.5g, 8.7±3.0 mos.) to determine the relative sensitivity of the admittance and conductance techniques to a contractility change induced by dobutamine infusion. Mice were anesthetized by administration of Urethane (1000 mg/kg IP) and Etomidate (25 mg/kg IP). Complex admittance (magnitude and phase) and conductance (magnitude

only) with left ventricular pressure were obtained at steady state and during occlusion of the IVC at both baseline and during administration of 5μg/kg/min of dobutamine through the jugular vein. Data acquisition for dobutamine was started 5 minutes after the initiation of the iv infusion. Volume data were calibrated using flow probe derived stroke volume at the end of each experiment, and subsequently converted to left ventricular volume using both Baan's equation, and Wei's equation. Parallel conductance G_P for Baan's equation was calculated as the constant mean value of the admittance-derived parallel conductance $G_P(t)$ to avoid blood conductivity changes due to the injection of hypertonic saline.

Determination of Epicardial Permittivity and Conductivity. A custom-designed epicardial probe [25] was applied to the surface of the intact beating open-chest murine heart of an additional n=7 mice and the stimulus current was generated using the instrumentation described above. Real-time $|\boldsymbol{Y}|$ and θ were measured and myocardial permittivity (ε_m) and conductivity (σ_m) were calculated as described previously [24, 25]. Briefly, the surface probe "cell constant", k (m^{-1}), determined in saline of known electrical conductivity, is used to calculate: $\sigma_m = k \cdot G_m$ and $\varepsilon_m = k \cdot C_m$, where $G_m = \mathrm{Re}\{\vec{Y}\}$ and $C_m = \mathrm{Im}\{\vec{Y}\}/\omega$ and $\omega = 2\pi f = 126$ krads/s.

Aortic Banded Mice. To investigate the impact of left ventricular hypertrophy on myocardial σ_m and ε_m, n=13 mice were studied (C57BlkS/J, female, age 5.1 ± 0.3 months) where n=6 mice underwent aortic banding for 1 week, and n=7 served as controls. Epicardial permittivity and conductivity were determined as described above. The echo study described above in the section "Admittance (Wei's equation) – Hypertonic Saline (Baan's equation) Comparison to Echo" above was repeated in these banded mice to determine the accuracy of the admittance technique with respect to echo. Traditional parallel conductance measurements were not repeated in this study to eliminate the conductivity change that occurs as a result of injection of hypertonic saline as a source of error.

Data Analysis.

Hypertonic Saline Technique. The instantaneously changing LV blood conductance in response to hypertonic saline injection was evaluated to determine the constant parallel conductance as described in Nielsen *et al.* [21]. Briefly, the relationship between the end-systolic conductance G_{ES} and the end-diastolic conductance G_{ED} can be described as $G_{ES} = m \times G_{ED} + b$. The point where the linear fit intersects the line of identity is the point where $G_{ES} = G_{ED}$, implying that the signal is completely derived from the myocardium. This single point (G_P) was used as an estimate of constant G_P for the entire experiment.

Traditional analysis based on Baan's equation was used to convert measured conductance into volume as previously described for intact murine hearts [11]. The constant α term is calculated to force the volume difference resulting from Baan's equation to be the same as an independently measured SV [30], i.e.

$$\alpha = \frac{\rho L^2 G_{B-ED} - \rho L^2 G_{B-ES}}{SV} . \quad (2)$$

The terms $G_{B\text{-}ED}$ and $G_{B\text{-}ES}$ are the blood conductances at end-diastole and end-systole, calculated by subtracting G_P from the conductance measured at end-diastole and end-systole. In the closed chest murine study, SV was computed using echo data in closed chest mice, and the same SV was applied to calibrate both Baan's equation and Wei's equation. Additionally, we performed a cuvette calibration and found that $\alpha = 1.01$ for the miniaturized PV catheter. Because in Baan's original description of α, and in many published studies [20] α is assumed to be 1, we calculated PV loops three ways with (a) $\alpha = 1$, (b) $\alpha(G_P)$ determined using Equation 6, and (c) α from SV calibration (as in Equation 2).

Admittance Technique.

Calibration. The catheter and instrument both produce an additional phase shift, because they introduce additional capacitance to the volume measurement. The key to separation of muscle and blood lies in the phase

measurement, so a calibration is performed to determine the phase contribution from these sources of artifact. The calibration performed allows quantification of both the catheter/instrument related phase, and their effects on admittance magnitude.

The admittance system is calibrated by measuring the admittance magnitude and phase angle of both the tetrapolar and epicardial catheters immersed in varying conductivity saline solutions (1000, 2000, 4000, 8000, 10000, and 12000 μS/cm). Saline is chosen for the calibration because it will not produce a measureable phase shift at this frequency. The range of conductivity of solutions is determined by including the smallest and largest values of conductivity expected in the *in vivo* mouse heart which ranges from 1600 μS/cm for myocardium to approximately 10000 μS/cm for blood. The admittance measurement is a parallel combination of the two. Thus, the admittance system phase calibration is designed to cover this entire range. The containers for the saline solutions are much greater in diameter than the distance between the voltage electrodes, so that the electric field produced by the current is essentially unconstrained by the sides of the container. The values measured for admittance magnitude and phase are therefore independent of the shape of the saline container, and only dependent on the catheter and measurement hardware.

Theory for Dynamic Parallel Conductance Removal Using Admittance. Instead of using hypertonic saline injection to determine the parallel conductance, we introduce the concept of a complex measurement of admittance ($\boldsymbol{Y}$). Our method makes use of the native capacitive properties unique to myocardium to identify its contribution to the measured signal so that it can be removed in real time without the need for hypertonic saline injection. The basis of measuring admittance (magnitude and phase) rather than conductance (magnitude only) is that at frequencies around f = 20 kHz, it has been shown that blood is purely resistive and has no measurable capacitance, but myocardium has both capacitive and resistive properties (Figure 2) [24, 25, 29]. This fact allows separation of the admittance of the myocardium from the combined admittance signal, using electric field theory.

For a vector electric field $\boldsymbol{E}$ in homogeneous tissue, the conductance and capacitance between the electrodes that establish the field are given by:

$$G = \frac{I}{V} = \frac{\iint_S \sigma_m \vec{E} \bullet d\vec{S}}{-\int_b^a \vec{E} \bullet d\vec{L}} = \sigma_m F \quad \text{, and} \tag{3}$$

$$C = \frac{Q}{V} = \frac{\iint_S \varepsilon_m \vec{E} \bullet d\vec{S}}{-\int_b^a \vec{E} \bullet d\vec{L}} = \varepsilon_m F \tag{4}$$

where: G = conductance (S), I = current (A), V = potential (V), σ = electrical conductivity (S/m), F = the field geometry factor (m), C = capacitance (F), and Q = charge (C). The integration is from one electrode to the other along a vector pathway, $\boldsymbol{L}$, and the surface, $\boldsymbol{S}$, encloses all of the current from the source electrode. For homogeneous tissue the measured conductance and capacitance are related by a simple ratio: $G = C\sigma/\varepsilon$. This is the central principle of our method. The important ratio of σ/ε is determined by a surface probe measurement, which is described in detail in [24].

Briefly, the imaginary part of the admittance is defined as $\mathrm{Im}\{\boldsymbol{Y}\} = |\boldsymbol{Y}|\sin(\theta) = \omega C_{myocardium} + \omega C_{catheter}$. Therefore, once the (purely imaginary) catheter contribution has been determined and subtracted through calibration in saline, $C_{myocardium} = |\boldsymbol{Y}|\sin(\theta) / \omega$. The real part of the admittance is $\mathrm{Re}\{\boldsymbol{Y}\} = |\boldsymbol{Y}|\cos(\theta) = G_{blood} + G_{myocardium}$ implying that $G_{blood} = |\boldsymbol{Y}|\cos(\theta) - C_{myocardium}\sigma/\varepsilon$. Based on these equations, we can determine the instantaneous values of parallel conductance, and blood conductance.

Wei's Conductance to Volume Equation. As described previously by Wei *et al.* [30], the relationship between conductance and volume should include a non-constant α term in any size heart because of the dynamically changing field shape. Wei's equation for converting conductance to volume is

$$Vol(t) = \frac{1}{\alpha(G_B)} \rho L^2 \cdot G_B \,, \tag{5}$$

where $\alpha(G_B)$ is a new time-varying expression for α, and G_B is the blood conductance ($G - G_P$) calculated as described above.

Wei describes α as dependent on the blood conductance G_B,

$$\alpha(G_B) = 1 - \frac{G_B}{\gamma} \,, \tag{6}$$

where γ is a constant described as

$$\gamma = \frac{-b \pm \sqrt{b^2 - 4ac}}{2a} \text{, where } \begin{aligned} a &= SV - \rho L^2 (G_{B-ED} - G_{B-ES}) \\ b &= -SV \cdot (G_{B-ED} + G_{B-ES}) \\ c &= SV \cdot G_{B-ED} \cdot G_{B-ES} \end{aligned} \,. \tag{7}$$

The larger positive solution for γ is used in all calculations. $G_{B\text{-}ED}$, $G_{B\text{-}ES}$, and SV are determined during steady state conditions, so while γ is constant, $\alpha(G_B)$ is dependent on G_B, which changes as the heart beats contrary to the constant α in Baan's equation.

Echocardiographic Calculations.

EDV and ESV. End-diastole was defined as coincident with the peak of the R wave on the ECG, and end-systole was defined as minimum LV volume. A long axis view was taken for both end-systole and end-diastole, and the volume measured was determined using the cardiac analysis package from the Vevo 770 software (VisualSonics, Toronto, Canada). We measured the long axis, and a single short axis within a long axis view

(see Figure 3A1 and B1), and assumed the second short axis to be of equal length. Volume was then computed using the prolate ellipse method. SV was determined as the difference between EDV and ESV, and was used in the calculation of both conductance and admittance derived LV volume.

Center and Off-Center Catheter Positions. Both center and off center positions were studied since placement of the miniaturized PV catheter across the aortic valve *in vivo* forces catheter placement near the septum and off the true LV center (Figure 1A, [23]). Thus, without echo guidance, the off center position is most often used by investigators.

To allow for comparison between a centered position and an off-center catheter position, the distance between the LV free-wall (LVFW) and the center of the catheter was measured, as was the distance between the center of the catheter and the septum (SEP). An example of these measurements is displayed in Figure 3A2 and B2. The percentage deviation from the center was calculated as

$$Dev = abs\left(1 - 2 \times \left(\frac{LVFW}{LVFW + SEP}\right)\right) \times 100\% \,. \tag{8}$$

In this calculation, a value of 100% indicates that the catheter position coincides with the inner myocardial wall, and a value of 0% indicates that the catheter is in the center of the ventricle. Catheter positions which are symmetric around the long axis result in the same percentage deviation from the center.

Statistical Analysis. EDV and ESV derived by Wei's equation using admittance $G_P(t)$ were compared with echo data for EDV and ESV at both the centered and off-center positions using a two-sample right-tailed student's t-test. All calculations were performed using Matlab software (The Mathworks Inc., Natick MA). EDV and ESV derived by Baan's equation using hypertonic saline G_P were also compared with echo data using the same methods at both the centered and off-center positions. These analyses are also presented as Bland-Altman plots. The enhancement in contractility in response to dobutamine between baseline and drug infusion

for both Baan's equation (SV calibration of α) and Wei's equation using admittance $G_P(t)$ were compared with student's t-test, and the alteration in myocardial properties between control and aortic banded mice were also compared with student's t-test.

III. Results

Non-banded Myocardial Properties Measurement. The conductivity and permittivity of myocardium were measured in a separate experiment in n=7 mice in an open chest preparation as described in [24]. All values are reported as mean ± standard deviation. The relative permittivity of myocardium derived from these measurements at 20 kHz was $\varepsilon_m = (11844 \pm 2700) * \varepsilon_0$ F/m, and the electrical conductivity of myocardium was measured at $\sigma_m = 0.160 \pm 0.046$ S/m. These results were used in calculations related to the admittance – conductance – echocardiography comparisons.

Hemodynamic and Echocardiographic Parameters for Admittance – Conductance Comparison. For n=8 mice, the body weight ranged from 19 to 30 g (mean = 26.5 ± 3.5 g), heart weight ranged from 85 to 152 mg (mean = 123.8 ± 21.2 mg), and LV weight ranged from 67 to 107 mg (mean = 90.8 ± 14.6 mg). The mean left ventricular peak systolic pressure was 102 ± 10 mmHg, and the heart rate was 407 ± 28 bpm. The mean echo end-diastolic volume was 40.9 ± 12.1 μl, and the mean echo end-systolic volume was 14.1 ± 5.5 μl. The echocardiographic SV used in the calculation of both alpha (α) and gamma (γ) had a mean value of 26.8 ± 7.2 μl.

The parallel conductance calculated by the hypertonic saline method was 476 ± 182 μS, and by the admittance technique ranged dynamically from 552 ± 79 μS at end-systole to 346 ± 67 μS at end-diastole. The mean off center α was 0.22 ± 0.15 as determined with echo SV, and it was 1.01 with cuvette. The mean γ was 1350 ± 389 μS. The location of the catheter position relative to the wall is shown in Table 1. The center technique was

closer to the true mid-line than the off-center position ($p < 0.0001$) based on the M-mode echo measurements. Typical examples of echo center and off-center catheter positions are shown in Figure 3.

Wei's Equation Using Admittance is More Accurate than Baan's Equation Using HS and Either SV or Cuvette Calibration With Off-Center Catheter Placement. The off-center derived PV loops from Wei's equation, Baan's equation with SV calibration ($\alpha = 0.22 \pm 0.15$), and Baan's equation with cuvette calibration ($\alpha = 1.01$) for all n=8 mice are shown in Figure 4. As is visually apparent in 5 of these 8 mice, the SV calibrated conductance derived PV loops are to the right of echo (mice # 2, 4, 5, 7, 8), and the cuvette calibrated conductance loops are to the left of echo (mice # 1, 2, 3, 6, 7). In contrast, all of the Wei's equation with admittance loops are similar to the echo derived volumes. The end-diastolic and end-systolic volumes derived using Wei's equation ($\alpha(G_B) \approx 0.7\text{-}0.9$) show significantly less absolute error (-2.49 ± 15.33 µl error ES and ED) than the same quantities calculated using SV calibrated conductance ($\alpha \approx 0.1\text{-}0.3$) (35.89 ± 73.22 µl error ES and ED) or cuvette calibrated conductance ($\alpha = 1$) (-29.10 ± 31.53 µl error ED, and -7.53 ± 16.23 µl error ES), taking the echo volumes as the standard of comparison ($p < 0.03$).

These results are shown in graphical format as Bland-Altman plots in Figure 5A. The Bland-Altman plot shows that most of the error lies in the low repeatability (high standard deviation) of measurements when relying on Baan's equation with SV calibration. A consistently small absolute volume and stroke volume are observable in results from Baan's equation with cuvette calibration, which is consistent with observations in the literature [14, 21]. These results show that when the catheter is not placed in an optimal, i.e., central position, admittance provides an advantage in accuracy.

Wei's Equation Using Admittance is as Accurate as Baan's Equation Using HS and SV or Cuvette Calibration with Centered Catheter Placement. For the same 8 mice, when the catheter was shifted to the central position and the same measurements were taken, the same trend was observed: every Wei's equation

using admittance PV loop was a smaller volume than those derived from Baan's equation $\alpha = 0.22 \pm 0.15$ with HS, and larger than every PV loop from Baan's equation $\alpha = 1.01$ using cuvette calibration (Figure 5). However, the difference in error between Wei's equation and echo measurement, and between both calibration methods for Baan's equation and echo, were not found to be statistically significant in either case with one exception: in the end diastolic measurements from cuvette calibration, Wei's equation shows lower error ($p < 0.03$). The closeness of these three results may be due to the removal of equivalent amounts of parallel conductance when the tetrapolar catheter is centered with echo guidance, where the average G_P using hypertonic saline is 476 ± 182 μS vs. admittance's average $G_P(t)$ of 448 ± 60 μS. The mean of an instantaneously varying parallel conductance and an example real-time signal are shown in Figure 6A. It is interesting to note that even though the difference among the results for the center position are not statistically significant, they still have much lower variance, as evidenced by the Bland-Altman plot in Figure 5.

Banded Mice. In an additional n=13 mice, the impact of left ventricular hypertrophy (aortic banding for 1 week, n=6) on myocardial properties was determined, compared to controls (n=7). Heart weight (86±4 mg control, 104±24 mg banded p=NS) and LV weight (70±7 mg control vs. 86±24 mg banded, p=NS) tended to increase with banding but not significantly due to the large standard deviation in the banded group. In banded mice, $\varepsilon_m = (21267 \pm 8005) * \varepsilon_0$ F/m, a significant increase in myocardial properties (11844 ± 2700 to 21267 ± 8005) * ε_0 F/m occurred compared to control ($p<0.05$). The myocardial conductivity showed no significant change between banded $\sigma_m = 0.200 \pm .080$ S/m and control $\sigma_m = 0.160 \pm 0.046$ S/m (p=NS) mice.

For the n=6 banded mice, the mean left ventricular peak systolic pressure was 157±30 mmHg and the heart rate was 471±67 bpm. The mean echo end-diastolic volume was 33.7 ± 11.0 μl, and the mean end-systolic volume was 12.9 ± 4.8 μl. The echocardiographic SV used in the calculation of gamma (γ) had a mean value of 20.8 ± 6.3 μl. The overall volume error compared to the echo standard was 6.74 ± 13.06 μl, which is

comparable to the error in the non-banded mice (-2.49 ± 15.33 μl), and less than the error for traditional conductance (35.89 ± 73.22 μl).

IVC Occlusions Show Dynamic Removal of a Non-Constant Parallel Conductance. In additional mice (n=4) IVC occlusions were performed to demonstrate the ability of the admittance technique to dynamically separate blood conductance and myocardium conductance. Figure 6A shows the typical separation of the blood and myocardial components during IVC occlusion in a single mouse using conductance and admittance techniques, and all four mice showed the same phenomenon. The observation from this figure, which represents a departure from traditional conductance theory, is that during an IVC occlusion the amount of myocardium in the sensing field increases while the blood component of conductance still decreases and dominates the total conductance signal. Traditional conductance methods assume a constant value for parallel conductance, which is demonstrated to be an inaccurate assumption by these data.

Preload reduction is commonly utilized to generate measures of left ventricular function such as the end-systolic elastance (E_{es}), diastolic chamber compliance, and others. We hypothesized that calculated values of E_{es} and other parameters would be affected by the change from traditional conductance with Baan's equation, to admittance with Wei's equation. Thus we analyzed the impact of these two techniques on calculated hemodynamic parameters for an identical transient occlusion of the inferior vena cava from a single mouse. Results are shown in Figure 6B. Despite the similarity in conductances in Figure 6C, the appearance of the loops in Figure 6B is significantly different.

Additionally, there was an increase in measures of contractility using the admittance technique. E_{es} rose from 3.4 to 15.4 mmHg/μl; maximum elastance rose from 12 to 25 mmHg/μl, preload recruitable stroke work rose from 52 to 95 mmHg·μl, conductance to admittance, respectively. Further, there was an increase in chamber stiffness from 0.061 sec^{-1} with conductance to 0.076 sec^{-1} by admittance.

Wei's Equation Using Admittance is more Sensitive to the Detection of Inotropic Stimulation. The hemodynamic response of n=6 mice were determined at baseline and following 5 minutes of steady state infusion of 5 μg/kg/min of iv dobutamine. Heart rate increased from 384 ± 47 to 523 ± 75 ($p<0.05$), respectively. P_{max} was unchanged from 97 ± 13 to 98 ± 11mm Hg, respectively (p=NS). dP/dt_{max} increased from 5,821 ± 1,802 to 12,309 ± 3,832 mm Hg sec^{-1}, respectively ($p<0.01$), and dP/dt_{min} decreased from -5,703 ± 1,491 to -7,505 ± 825 mm Hg sec^{-1}, respectively ($p<0.05$).

To evaluate the impact on parameters derived using Wei's equation and Baan's equation (both using SV calibration) during the identical IVCO, linear E_{es} and dP/dt-EDV were determined in these same mice. E_{es} increased from 4.9 ± 1.4 to 12.5 ± 6.6 using Wei's equation ($p<0.05$), and from 3.3 ± 1.2 to 8.8 ± 5.1 $mmHg \cdot \mu l^{-1}$ using Baan's equation (p=NS). A representative example is shown in Figure 7. Similarly, the dP/dt – EDV relationship increased from 158 ± 127 to 542 ± 320 using admittance ($p<0.05$), and from 117 ± 78 to 263 ± 123 mmHg sec^{-1} μl^{-1}using Baan's equation (p=NS).

IV. Discussion

The current study compares the V(t) determined by Baan's equation using G_P from HS with SV or cuvette calibration, to V(t) determined by Wei's equation using admittance. We have demonstrated (1) more accurate volumes with Wei's equation using admittance when the catheter is in the off-center position than Baan's equation using SV or cuvette calibration, (2) that the parallel conductance, G_P, varies between end-systole and end-diastole, and even more significantly during IVC occlusion, (3) the advantages of using a dynamically-changing α which is dependent on $G_B(t)$, (4) improved sensitivity in the detection of inotropic stimulation with Wei's equation and $G_P(t)$ calculated using admittance, compared to Baan's equation and G_P calculated using HS with SV calibration of α, (5) demonstration that the myocardial properties change with left ventricular hypertrophy, and (6) demonstration that the improved accuracy of admittance in the determination of LV volumes extends to mice with aortic banding.

406 **Dynamic Parallel Conductance Calculation.** In an early study by Lankford *et al*., parallel conductance was
407 demonstrated to be a constant between end-diastole and end-systole [18]. Historically, this study was the
408 theoretical basis for the acceptance of hypertonic saline injection determination of G_P in the literature. However,
409 myocardium has a both a conductive and a dynamic capacitive component [25, 30, 31]. This concept is not
410 reflected in the assumptions or conclusion of Lankford's study, nor in any traditional conductance technique
411 where phase is not measured [1, 2, 8, 10, 11, 21, 26]. Mathematically speaking, the G_P calculated using
412 admittance is a closer approximation to the true value of G_P than traditional conductance because it takes into
413 account the complex nature of myocardium $\boldsymbol{Y}_P = G_P + j\omega C_P$, and therefore includes measurable changes during
414 the cardiac cycle. The current results (Figure 6A) and our previous study [30] imply that parallel conductance is
415 changing even between end-diastole and end-systole, as predicted by electric field theory [31].

416 **Calculation of the Gain Term α.** In the early conductance literature, the value of α was not calculated. α was
417 assumed to be equal to 1, as described by Baan *et al* [2] and more recently by Uemura *et al* [28]. The purpose of
418 the term α is to calibrate the stroke volume of the resulting conductance signal to match a standard of
419 comparison (usually a flow probe, or echo). However, because α is dependent on the field geometry, and field
420 geometry is constantly changing throughout the cardiac cycle, α is not a constant. As shown in Figure 8 during
421 an IVC occlusion in a single mouse, the value of α is different depending on which calibration method is used.
422 For example, using Wei's equation, the dynamic nature of α is evident both between systole and diastole, and
423 down the IVC occlusion ramp. In contrast, both other calibration procedures using flow or echo calibration (α =
424 0.79 for centered position) and the volume cuvette method ($\alpha = 1$) recommended by manufacturers of the
425 currently used commercial mouse conductance systems, both use a constant value for α. The impact of using a
426 variable α is that the volume equation will more closely model the changes which the field sees, as opposed to
427 assuming a constant shape of the electric field.

Limitations of Cuvette Calibration. Review of the literature (122 publications) revealed that 63% of murine conductance studies utilize the volume cuvette as the calibration method of choice to directly convert voltage to absolute volume [20]. However, recent studies [14, 21] have shown that cuvette-calibrated left-ventricular volumes are consistently smaller than those derived with a standard such as MRI, confirmed as well in the current study. Volume cuvettes have an electrically insulating boundary at the myocardial wall, which cramps the field causing an artificially high value of α (implying a small stroke volume). This high value of α causes small resultant volumes, and small resultant stroke volumes (See Figure 4).

Limitations of a constant α. A correction for the SV error introduced by the volume cuvette is to force the final SV to be the same as an independent measure. However, forcing only the SV to the independently verified value in an off-center position will reduce the value of α, increasing the "gain factor" (α^{-1}) of the volume equation. The benefit to the conductance technique is an accurate SV, but the detriment is an inflation of all volumes. As shown in Figure 4, although all SV are more physiologic when $\alpha = 0.22 \pm 0.15$, in mouse #2, 7, and 8, there is an inflation of volumes to an unphysiologic value. Although Figure 4 was generated from the off-center position of the miniaturized PV catheter, this is often the location of catheter in the heart without echo guidance, since the aortic valve is off-center relative to the middle of the LV chamber.

Dynamically Changing α (Wei's Equation). The advantage of using a dynamic value for α is that more realistic volumes are obtained. As shown in Figure 4, incorporating a dynamic value for α provided absolute volumes closest to the echo standard. Wei's equation provides a nonlinear conductance to volume relationship which has been noted in some recent papers [21]. However, the most significant improvement is that Wei's $\alpha(G_B)$ is a function of blood conductance G_B (see Equation 6) and γ. The derived value, γ, represents the value of conductance at saturation (where the catheter is placed in an arbitrarily large pool of conductive solution), so the expression $\alpha(G_B)$ incorporates the changing geometry of the electric field as the heart beats. This advantage

of the γ-formulation will be particularly important when performing changes in loading conditions, such as IVC occlusion.

Wei's Equation Using Admittance $G_P(t)$ Improves Volume Estimates for Off-Center Placement of the PV Catheter. One assumption of Baan's equation is that the tetrapolar catheter is placed in the center of the left ventricle. However, the off center location of the aortic valve relative to the mid-LV chamber in mammalian hearts forces the miniaturized PV catheter to be closer to the septum (Figure 1A, [23]). Only the use of an independent imaging modality, such as echo, will allow a miniaturized PV catheter to be moved closer to the true center of the LV. Echocardiography, however, is not routinely used to center the conductance catheter. In the current study, despite the use of echo guidance, the mean central placement was actually 14 $\pm$ 9% at end-diastole, where 0% was true center and 100% is the endocardium or septum. In addition, as the heart moves, one cannot assume that the catheter position stays at the midline. Some investigators estimate that the catheter shifts by 50-70% of the ventricular radius [17]. Thus, placement of the tetrapolar catheter in an off-center position is a common source of error.

In the present study, the off-center tetrapolar catheter Wei's equation using admittance $G_P(t)$ show statistically less error than traditional conductance measurements taken simultaneously in a closed chest mouse, with simultaneous high frequency echocardiography used as the standard for true left ventricular volume. One explanation is that admittance provides a measure of instantaneous parallel conductance while all previous methods cannot. This is particularly evident in Figure 6A, during occlusion of the inferior *vena cava*, where the myocardial component of the admittance signal is shown to vary both between end-diastole and end-systole, as well as during the occlusion ramp.

Additionally, the use of a dynamic value for α that is dependent on the value of conductance shows a more physiologic range for the absolute volume, while still matching the stroke volume of an independent method (usually flow probe or echo). In Baan's equation, the α term is dependent only on the conductance-derived SV.

In Wei's equation however, the $\alpha(G_B)$ term is dependent on both the SV, and the current values of conductance. Figure 6B and Figure 6C demonstrate that this conclusion is only in part due to the differences in parallel conductance removal. In addition, the calculated volume ranges are quite different in Figure 6B, while the conductances shown in Figure 6C are similar, implying that the difference in the volumes is due to a difference in α as well.

As with any linear relationship, the slope α and the y-intercept G_P, are the only two points of control for the calibration of the volume signal using Baan's equation. This makes the accuracy of Baan's equation dependent on obtaining the correct value of G_P (which magnifies problems of using a constant α) and correct value of parallel conductance determined with hypertonic saline (which has a high relative error in the mouse) [2, 10].

The hypertonic saline estimate of parallel conductance is complicated in the mouse by: 1) changes in stroke volume caused by preloading the heart with the volume of hypertonic saline injected, 2) changes in blood electrical conductivity due to multiple injections (usually averaged), 3) variability in the manner of the injection (volume, rate, etc.), and 4) extrapolation of data to the line of identity. The variability of the hypertonic saline technique explains why in Figure 4 some SV calibrated conductance-derived loops are close to echo standard, while others substantially overestimate echo standard end-systolic volumes. Specifically, there are examples in Figure 4 where the traditional conductance-derived LV volumes are similar to echo standard (mice 1,3,6). However, other examples in the same figure demonstrate conductance-derived end-systolic volumes that overestimate the echo standard (mice 2,4,5,7,8). In mice 1,3,6 the hypertonic saline technique reports parallel conductance values (623 ± 65 μS) which are significantly higher ($p < 0.01$) than in mice 2,4,5,7,8 (389 ± 114 μS). Consequently, mice 1,3,6 have traditional conductance-calculated absolute LV volumes, specifically the end-systolic volume, closer to the truth because subtraction of a larger parallel conductance moves the volume

to a more realistic range. In contrast, mice 2,4,5,7,8 have significantly smaller parallel conductance subtracted leaving the final calculated volumes larger than the echo standard.

Importance of Myocardial Properties Measurement. The current study demonstrates that the permittivity (ε_m) increases with LV hypertrophy induced by aortic banding for 1 week, while the myocardial conductivity (σ_m) did not change significantly. It is known that larger myocytes have a greater membrane capacitance [12]. The measurement of capacitance in the electrode field is increasing during LV hypertrophy, thus a higher permittivity is inferred from the measurement. In our bulk tissue measurement, the increased permittivity detected is likely a summation of this basic property. Thus, it is critical to measure this σ/ε ratio in every group of mice with myocardial disease if our technique is to derive LV volume accurately.

Limitations and Future Work. The ability of admittance to detect instantaneous parallel conductance should provide different measures of hemodynamic endpoints derived in the pressure-volume plane, although not having a standard measure of, for instance, end-systolic elastance (E_{es}), it is not clear how this advantage can be proven, other than the data shown in Figures 6B and 7. Further, our results question the accuracy of absolute values of hemodynamic parameters determined through the pressure – volume plane, such as E_{es}. Although relative changes in E_{es} are accurate, the absolute value of E_{es} determined using traditional conductance theory would be different than those derived from admittance down an IVC occlusion ramp. Admittance has the capability to detect and remove, in real time, this dynamic interaction between the electric field and myocardium as the heart shrinks in size on a beat-by-beat basis.

While admittance has the same physical significance in larger hearts, it is not clear at this point if the improvement in accuracy will be statistically significant in larger animals. Similar to conductance measurements, admittance scales with the size of the catheter (because of the length "L" between the voltage electrodes in Baan's equation), so larger lead spacing can be used to measure larger volumes without the concern of saturating the admittance measurement. Also, multi-electrode catheter theory is compatible with

admittance calculations, as the total admittance between two or more adjacent pairs of sensing electrodes is equal to the sum of the pairs. We plan to extend our studies to larger animals in the future to explore these issues.

V. Conclusion

We conclude that for closed-chest mice, admittance (dynamic G_P) and Wei's equation (dynamic α) provide more accurate volumes than traditional conductance, are more sensitive to inotropic changes, eliminate the need for hypertonic saline, and can be accurately extended to aortic banded mice.

VI. Acknowledgements

The studies presented in this paper were supported with tetrapolar micromanometer catheters supplied from Scisense, Inc. (London, Ontario, Canada). The authors would also like to thank Dr. G. Patricia Escobar for her help with echo data acquisition, and Jason Hansen for assistance with pressure-volume analysis.

VII. Grants

Supported with grants from the VA Merit (MDF), NIH (R21 HL079926)

X. References

[1] **Baan J, Jong TT, Kerkhof PL, Moene RJ, van Dijk AD, van der Velde ET, Koops J.** Continuous stroke volume and cardiac output from intra-ventricular dimensions obtained with impedance catheter. *Cardiovasc Res*, 15(6):328–334, Jun 1981.

[2] **Baan J, van der Velde ET, deBruin HG, Smeenk GJ, Koops J, van Dijk AD, Temmerman D, Senden J, Buis B.** Continuous measurement of left ventricular volume in animals and humans by conductance catheter. *Circulation*, 70(5):812–823, Nov 1984.

[3] **Bergman MR, Teerlink JR, Mahimkar R, Li L, Zhu B, Nguyen A., Dahi S, Karliner JS, Lovett DH.** Cardiac matrix metalloproteinase-2 expression independently induces marked ventricular remodeling and systolic dysfunction. *Am J Physiol Heart Circ Physiol*, 292(4):H1847–H1860, Apr 2007.

[4] **Claessens TE, Georgakopoulos D, Afanasyeva M, Vermeersch SJ, Millar HD, Stergiopulos N, Westerhof N, Verdonck PR, Segers P.** Nonlinear isochrones in murine left ventricular pressure-volume loops: how well does the time-varying elastance concept hold? *Am J Physiol Heart Circ Physiol*, 290(4):H1474–H1483, Apr 2006.

[5] **Costandi PN, Frank LR, McCulloch AD, Omens JH.** Role of diastolic properties in the transition to failure in a mouse model of the cardiac dilatation. *Am J Physiol Heart Circ Physiol*, 291(6):H2971–H2979, Dec 2006.

[6] **Feldman MD, Erikson JM, Mao Y, Korcarz CE, Lang RM, Freeman GL.** Validation of a mouse conductance system to determine LV volume: comparison to echocardiography and crystals. *Am J Physiol Heart Circ Physiol*, 279(4):H1698–H1707, Oct 2000.

[7] **Feldman MD, Mao Y, Valvano JW, Pearce JA, Freeman GL.** Development of a multifrequency conductance catheter-based system to determine lv function in mice. *Am J Physiol Heart Circ Physiol*, 279(3):H1411–H1420, Sep 2000.

[8] **Gawne TJ, Gray KS, Goldstein RE.** Estimating left ventricular offset volume using dual-frequency conductance catheters. *J Appl Physiol*, 63(2):872–876, Aug 1987.

[9] **Georgakopoulos D, Kass DA.** Minimal force-frequency modulation of inotropy and relaxation of in situ murine heart. *J Physiol*, 534(Pt. 2):535–545, Jul 2001.

[10] **Georgakopoulos D, Kass DA.** Estimation of parallel conductance by dual-frequency conductance catheter in mice. *Am J Physiol Heart Circ Physiol*, 279(1):H443–H450, Jul 2000.

[11] **Georgakopoulos D, Mitzner WA, Chen CH,. Byrne BJ, Millar HD, Hare JM, Kass DA.** In vivo murine left ventricular pressure-volume relations by miniaturized conductance micromanometry. *Am J Physiol*, 274(4 Pt 2):H1416–H1422, Apr 1998.

[12] **Hille, B.** The membrane as a capacitor. In: *Ion Channels of Excitable Membranes, Third Edition*. Sunderland, MA: Sinauer Associates Inc., 2001.

[13] **Ikonomidis JS, Hendrick JW, Parkhurst AM, Herron AR, Escobar PG, Dowdy PB, Stroud RE, Hapke E, Zile MR, Spinale FG.** Accelerated lv remodeling after myocardial infarction in timp-1-deficient mice: effects of exogenous mmp inhibition. *Am J Physiol Heart Circ Physiol*, 288(1):H149–H158, Jan 2005.

[14] **Jacoby C, Molojavyi A, Flögel U, Merx MW, Ding Z, Schrader J.** Direct comparison of magnetic resonance imaging and conductance microcatheter in the evaluation of left ventricular function in mice. *Basic Res Cardiol*, 101(1):87–95, Jan 2006.

[15] **Joho S, Ishizaka S, Sievers R, Foster E, Simpson PC, Grossman W.** Left ventricular pressure-volume relationship in conscious mice. *Am J Physiol Heart Circ Physiol*, 292(1):H369–H377, Jan 2007.

[16] **Jung AS, Harrison R, Lee KH, Genut J, Nyhan J, Brooks-Asplund EM, Shoukas AA, Hare JM, Berkowitz DE.** Simulated microgravity produces attenuated baroreflex-mediated pressor, chronotropic, and inotropic responses in mice. *Am J Physiol Heart Circ Physiol*, 289(2):H600–H607, Aug 2005.

[17] **Kun S, Peura RA.** Analysis of conductance volumetric measurement error sources. *Med Biol Eng Comput*, 32(1):94–100, Jan 1994.

[18] **Lankford EB, Kass DA, Maughan WL, Shoukas AA.** Does volume catheter parallel conductance vary during a cardiac cycle? *Am J Physiol*, 258(6 Pt 2):H1933–H1942, Jun 1990.

[19] **Li M, Georgakopoulos D, Lu G, Hester L, Kass DA, Hasday J, Wang Y.** p38 map kinase mediates inflammatory cytokine induction in cardiomyocytes and extracellular matrix remodeling in heart. *Circulation*, 111(19):2494–2502, May 2005.

[20] **Millar Instruments.** Published papers: Pressure - mouse / rat. [Online]. Available: http://www.millarinstruments.com/papers/papers_pres_m_r.php, 2008. Accessed: Aug. 21, 2008.

[21] **Nielsen JM, Kristiansen SB, Ringgaard S, Nielsen TT, Flyvbjerg A, Redington AN, Bøtker HE.** Left ventricular volume measurement in mice by conductance catheter: evaluation and optimization of calibration. *Am J Physiol Heart Circ Physiol*, 293(1):H534–H540, Jul 2007.

[22] **Pacher P, Bátkai S, Osei-Hyiaman D, Offertáler L, Liu J, Harvey-White J, Brassai A, Járai Z, Cravatt BF, Kunos G.** Hemodynamic profile, responsiveness to anandamide, and baroreflex sensitivity of mice lacking fatty acid amide hydrolase. *Am J Physiol Heart Circ Physiol*, 289(2):H533–H541, Aug 2005.

[23] **Pacher P, Nagayama T, Mukhopadhyay P, Bátkai S, Kass DA.** Measurement of cardiac function using pressure-volume conductance catheter technique in mice and rats. *Nat Protoc*, 3(9):1422–1434, 2008.

[24] **Raghavan K, Porterfield JE, Kottam ATG, Feldman MD, Escobedo D, Valvano JW, Pearce JA.** Electrical conductivity and permittivity of murine myocardium. *IEEE Trans Biomed Eng*, 2008.

[25] **Reyes M, Steinhelper ME, Alvarez JA, Escobedo D, Pearce JA, Valvano JW, Pollock BH, Wei C, Kottam A, Altman D, Bailey S, Thomsen S, Lee S, Colston JT, Oh JH, Freeman GL, Feldman MD.** Impact of physiological variables and genetic background on myocardial frequency-resistivity relations in the intact beating murine heart. *Am J Physiol Heart Circ Physiol*, 291(4):H1659–H1669, Oct 2006.

[26] **Steendijk P, Mur G, Van Der Velde ET, Baan J.** The four-electrode resistivity technique in anisotropic media: theoretical analysis and application on myocardial tissue in vivo. *IEEE Trans Biomed Eng*, 40(11):1138–1148, Nov 1993.

[27] **Takimoto E, Belardi D, Tocchetti CG, Vahebi S, Cormaci G, Ketner EA, Moens AL, Champion HC, Kass DA.** Compartmentalization of cardiac beta-adrenergic inotropy modulation by phosphodiesterase type 5. *Circulation*, 115(16):2159–2167, Apr 2007.

[28] **Uemura K, Kawada T, Sugimachi M, Zheng C, Kashihara K, Sato T, Sunagawa K.** A self-calibrating telemetry system for measurement of ventricular pressure-volume relations in conscious, freely moving rats. *Am J Physiol Heart Circ Physiol*, 287(6):H2906–H2913, Dec 2004.

[29] **Wei C, Valvano JW, Feldman MD, Nahrendorf M, Peshock R, Pearce JA.** Volume catheter parallel conductance varies between end-systole and end-diastole. *IEEE Trans Biomed Eng*, 54(8):1480–1489, Aug 2007.

[30] **Wei C, Valvano JW, Feldman MD, Pearce JA.** Nonlinear conductance-volume relationship for murine conductance catheter measurement system. *IEEE Trans Biomed Eng*, 52(10):1654–1661, Oct 2005.

[31] **White PA, Redington AN.** Right ventricular volume measurement: can conductance do it better? *Physiol Meas*, 21(3):R23–R41, Aug 2000.

[32] **Yue P, Arai T, Terashima M, Sheikh AY, Cao F, Charo D, Hoyt G, Robbins RC, Ashley EA, Wu J, Yang PC, Tsao PS.** Magnetic resonance imaging of progressive cardiomyopathic changes in the db/db mouse. *Am J Physiol Heart Circ Physiol*, 292(5):H2106–H2118, May 2007.

X. FIGURE LEGEND

Figure 1: Block diagram of the admittance instrument.

Figure 2: A simplified diagram to explain how phase (θ) is measured is shown. The conductance electrodes are demonstrated as planar metal electrodes surrounding homogenous media of either blood, myocardium, or both. The solid line is input current (μA), and the dotted line is output voltage (mV): **A.** Measurement of blood only, provides no phase shift θ. **B.** Combination of blood and muscle has some phase θ, and a somewhat larger amplitude output voltage (implying lower total admittance magnitude, ***Y*** = I/V). **C.** Pure muscle results in the largest phase shift θ and largest amplitude output voltage (low admittance magnitude). Phase measurement allows the separation of blood and muscle (**B**) in real time.

* The phase shift is exaggerated in this figure to emphasize relative difference.

Figure 3: A. Center positioned catheter guided by echo. **A1.** Long axis view **A2.** M-Mode view. **B.** Off-center positioned catheter guided by echo. **B1.** Long axis view **B2.** M-Mode view. M-Mode views quantify catheter to myocardium distances in mm. White double-headed arrows in long axis view indicate the line of M-Mode measurement.

Figure 4: Pressure-Volume loops from mice with catheter positioned off-center. The solid lines represent the end-systolic and end-diastolic echo reference. The solid loops were derived with Wei's equation and admittance where $\alpha(G_B(t))$ is determined instantaneously, and ranges between 0.7 and 0.9 during the cardiac cycle; the dot-dash loops were derived using Baan's method of hypertonic saline with cuvette calibration ($\alpha = 1$); the dash loops were derived using Baan's method of hypertonic saline with echo SV calibration ($\alpha = 0.1 – 0.3$). As is visually evident, the admittance technique in combination with Wei's equation was closer to echo.

Figure 5: The volume difference of each method vs. echo is plotted on the y-axis vs. the mean of echo and each method on the x-axis in these Bland Altman plots in n=8 mice for both End-Systolic (circle) and End-Diastolic (x) volume measured at **A.** the off-center position comparing **A1.** Volume from Baan's Equation using

hypertonic saline vs. Echo volume (Average Error for ESV = -7.54 ± 16.23 µl, and EDV = -29 ± 15.33 µl), **A2.** Volume from Wei's Equation using admittance vs. echo volume, (Average Error for ESV and EDV are equivalent, Error = -2.49 ± 15.33 µl), **A3.** Volume from Baan's Equation with echo SV calibration using hypertonic saline (Average Error for ESV and EDV are equivalent, Error =35.89 ± 73.22 µl); and **B.** the same three plots with the catheter at the center position. **B1.** Average error for cuvette-calibrated conductance ESV = -7.54 ± 16.23 µl, and EDV = -29 ± 15.33 µl **B2.** Average error for Admittance ESV and EDV are equivalent, Error = -6.64 ± 24.3 µl. B3. Average error for SV-calibrated conductance ESV and EDV are equivalent, Error = -20.96 ± 38.42 µl

Solid lines represent means and dashed lines represent the 95% confidence intervals. †Less error than SV-calibrated conductance ($p < 0.03$ in a student's t-test). ‡Less error than cuvette-calibrated conductance ($p<0.03$)

Figure 6: Example data from a single mouse during an identical preload reduction analyzed by constant G_P subtraction with Baan's equation (SV calibration of α), and admittance with Wei's equation are shown. **A.** The dynamic parallel conductance (G_M) computed by the admittance technique, is contrasted with the constant G_M subtracted by the conductance technique. The corrected conductance of blood (G_B) from admittance technique is also shown for reference. **B.** The data demonstrate differences in volumes and measures of contractility ESPVR for conductance $P_{ES} = 3.360 \cdot (V_{ES} – 0.942)$, and admittance $P_{ES} = 15.425 \cdot (V_{ES} – 15.566)$. Also shown are the EDPVR for conductance $P_{ED} = 4.797 \cdot 10^{-1} \cdot \exp(0.061 \cdot V_{ED})$ and admittance, $P_{ED} = 7.366 \cdot 10^{-1} \cdot \exp(0.076 \cdot V_{ED})$ **C.** The corrected conductance signals derived when admittance is used (a dynamic removal of parallel conductance), vs. conductance (a constant removal of parallel conductance).

Figure 7: Representative example demonstrating that admittance (with Wei's equation, upper panel) is more sensitive in the detection of an increase in inotropy in response to iv dobutamine than Baan's equation (SV calibration of α, lower panel) during the identical IVCO in a single mouse. Similar results were found in n=6 mice (see text for discussion).

668 **Figure 8:** α plotted versus time from each of the three calibration methods during the same IVC occlusion as
669 Figure 6. The dynamic nature of Wei's α is demonstrated to be in contrast with constant α as derived with either
670 the cuvette or SV calibrated conductance techniques (using a flow probe to determine SV to calculate α).
671

672 ## XI. TABLE LEGEND

673 **Table 1:** Catheter position for each mouse. *Percentages represent positional deviation from center. 0% =
674 center, 100% = wall. See Equation 8 for calculation of percentage.
675
676

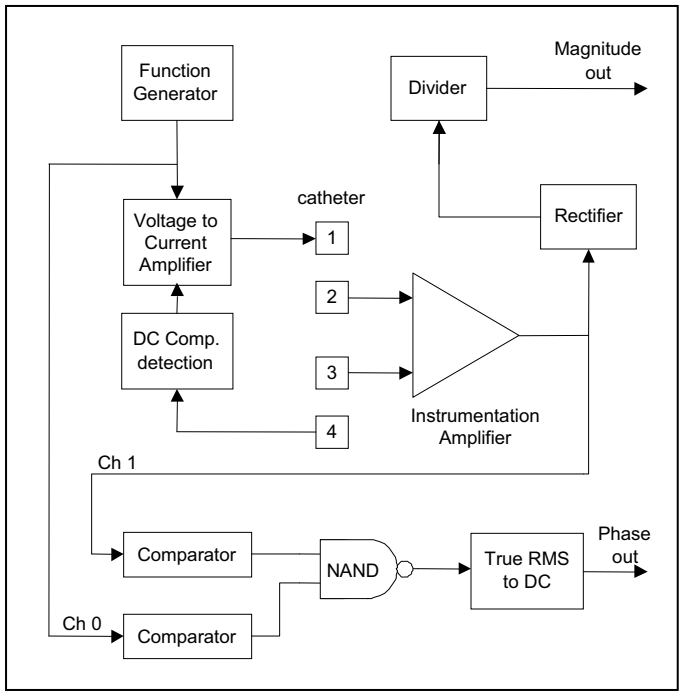
Function Generator
Divider
Magnitude out
catheter
Voltage to Current Amplifier
Rectifier
1
2
3
4
DC Comp. detection
Instrumentation Amplifier
Ch 1
Comparator
NAND
True RMS to DC
Phase out
Ch 0
Comparator

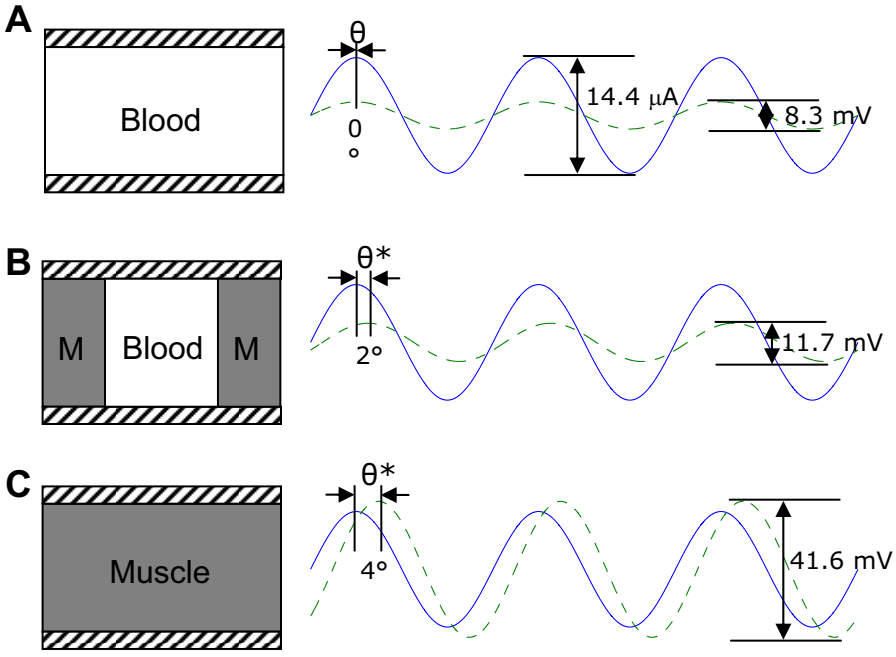
A
Blood
θ
0
°
14.4 μA
8.3 mV
B
M
Blood
M
θ*
2°
11.7 mV
C
Muscle
θ*
4°
41.6 mV

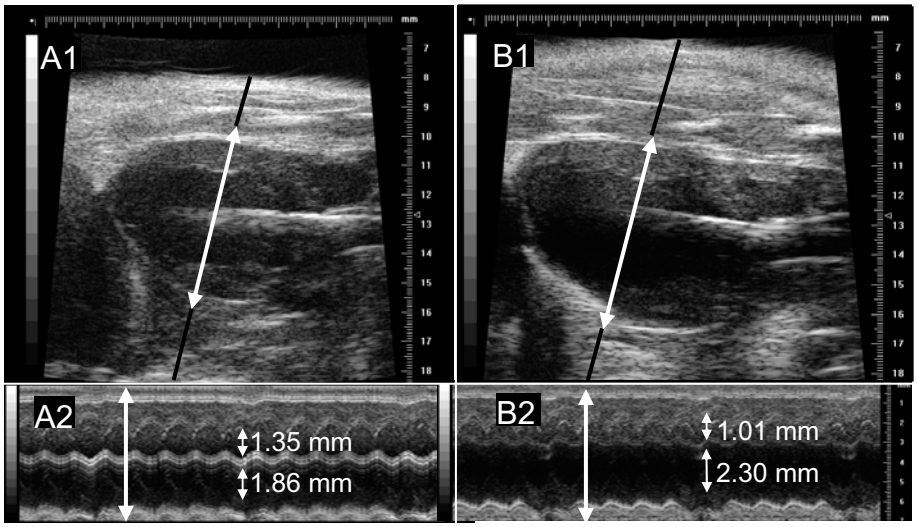
A1
B1
A2
1.35 mm
1.86 mm
B2
1.01 mm
2.30 mm

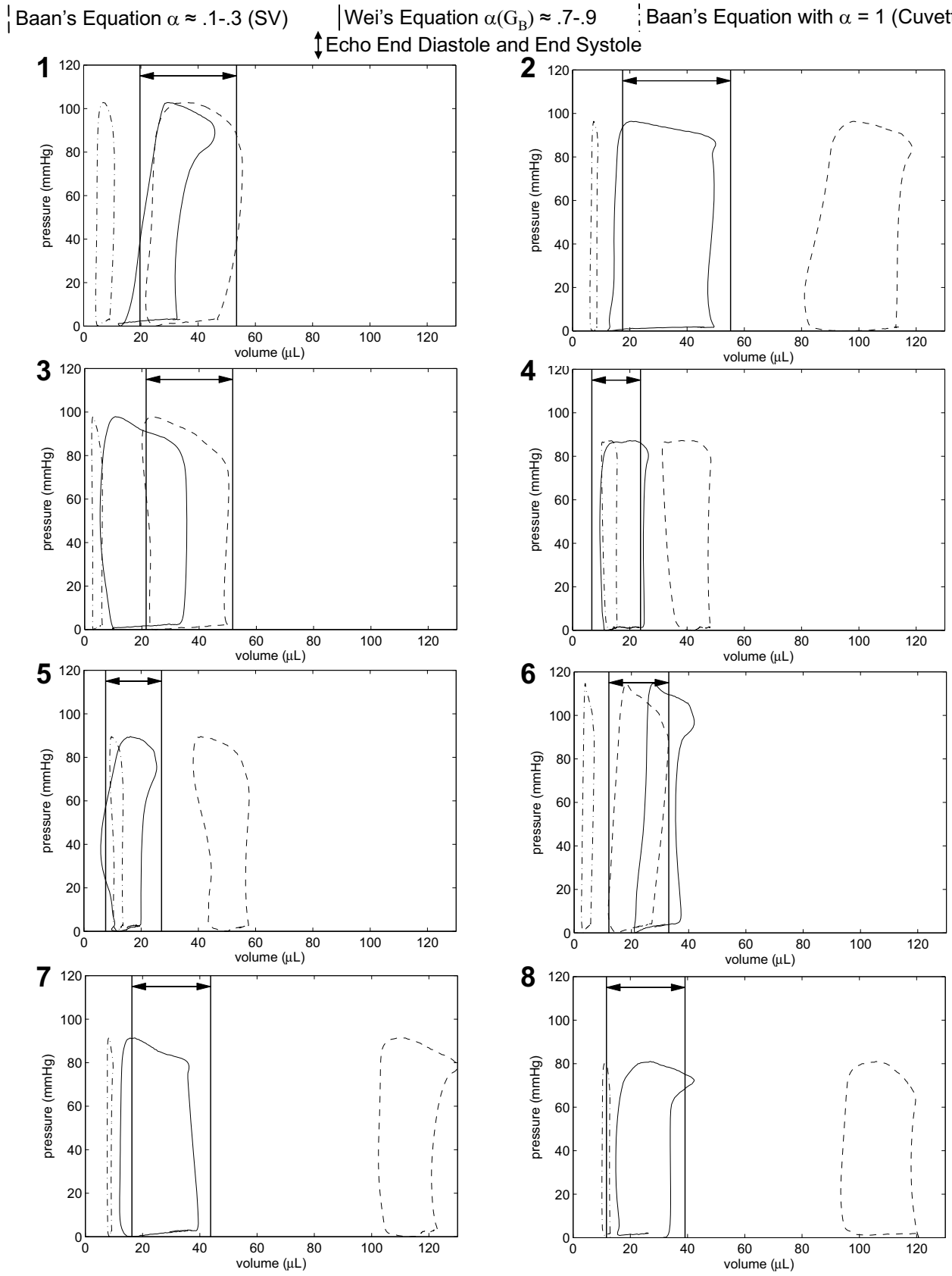
Baan's Equation α ≈ .1-.3 (SV)
Wei's Equation α(G_B) ≈ .7-.9
Baan's Equation with α = 1 (Cuvette)
Echo End Diastole and End Systole
1
2
3
4
5
6
7
8
pressure (mmHg)
volume (μL)

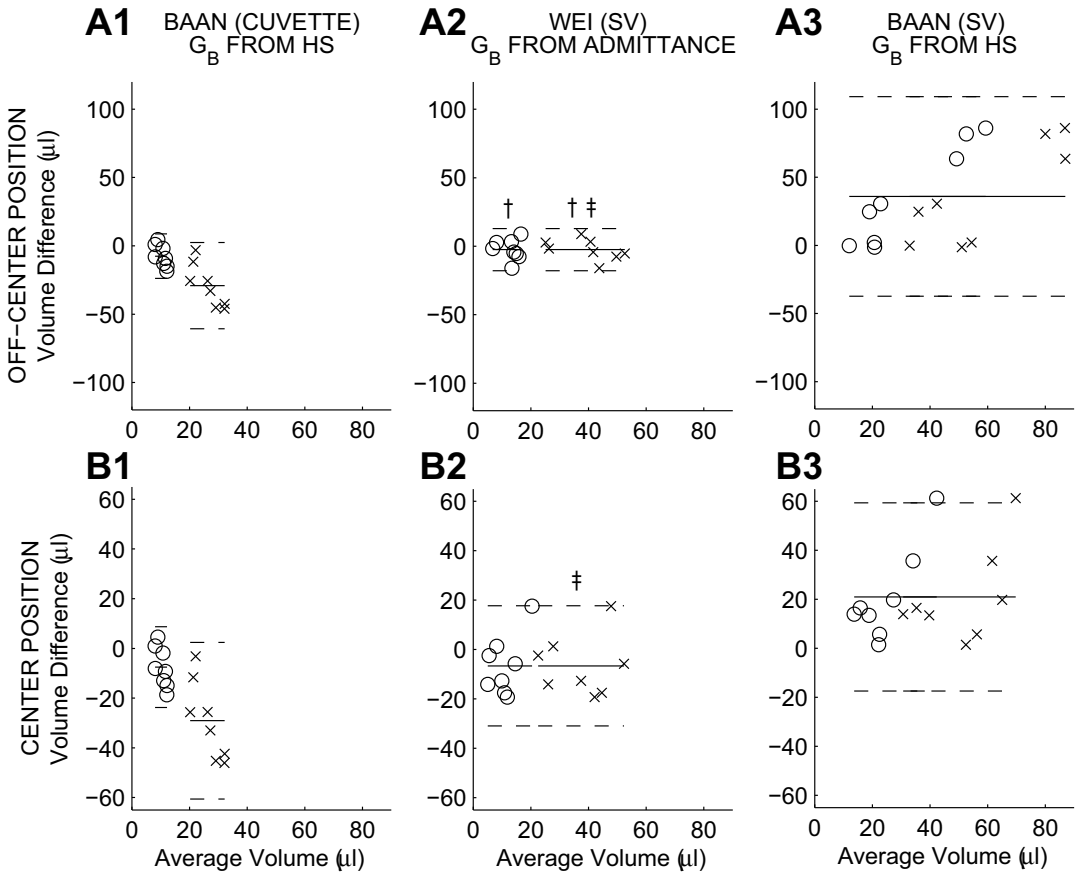
A1
BAAN (CUVETTE)
G_B FROM HS
A2
WEI (SV)
G_B FROM ADMITTANCE
A3
BAAN (SV)
G_B FROM HS
OFF−CENTER POSITION
Volume Difference (µl)
B1
B2
B3
CENTER POSITION
Volume Difference (µl)
Average Volume (µl)
Average Volume (µl)
Average Volume (µl)

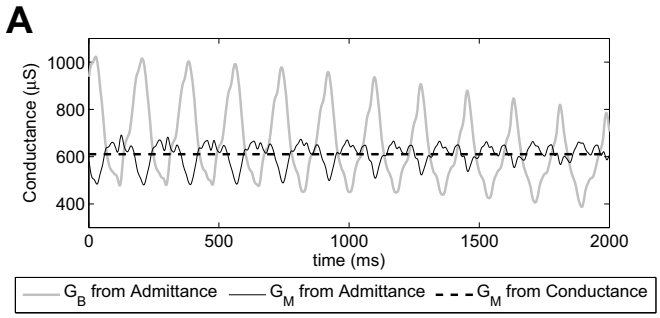
A
Conductance (μS)
1000
800
600
400
0
500
1000
1500
2000
time (ms)
G_B from Admittance
G_M from Admittance
G_M from Conductance

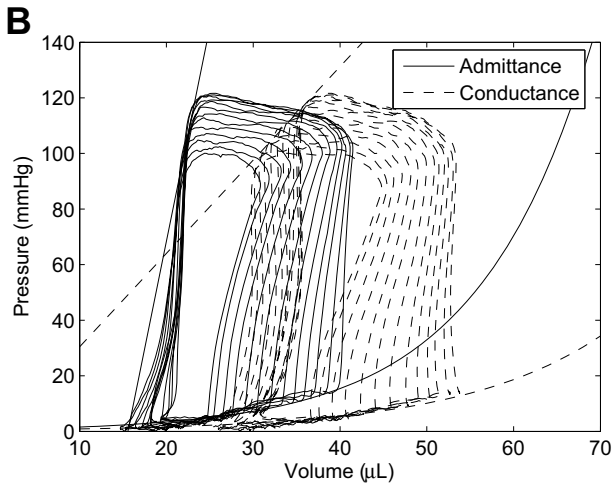
B
Admittance
Conductance
Pressure (mmHg)
140
120
100
80
60
40
20
0
10
20
30
40
50
60
70
Volume (μL)

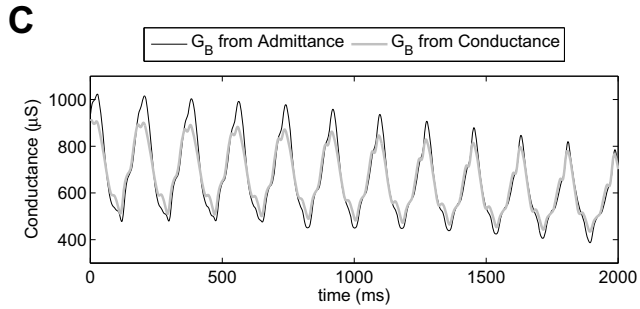
C
G_B from Admittance
G_B from Conductance
Conductance (μS)
1000
800
600
400
0
500
1000
1500
2000
time (ms)

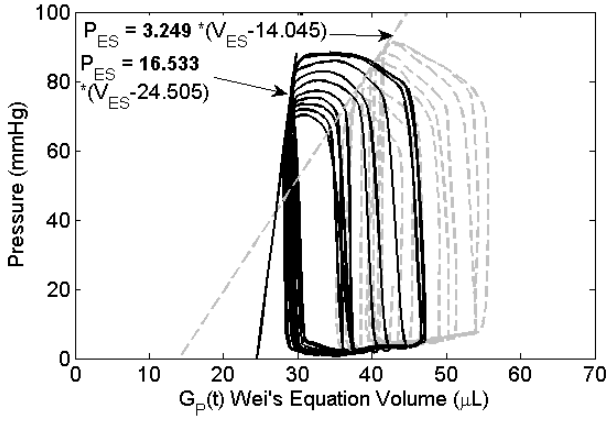
P_ES = 3.249 *(V_ES-14.045)
P_ES = 16.533 *(V_ES-24.505)
Pressure (mmHg)
G_P(t) Wei's Equation Volume (μL)
0
20
40
60
80
100
0
10
20
30
40
50
60
70

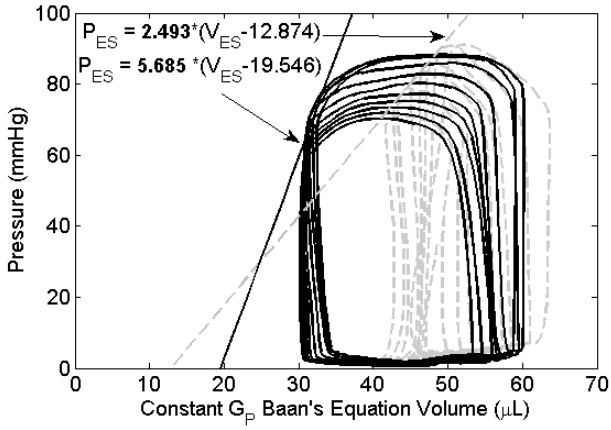
P_ES = 2.493*(V_ES-12.874)
P_ES = 5.685 *(V_ES-19.546)
Pressure (mmHg)
Constant G_P Baan's Equation Volume (μL)
0
20
40
60
80
100
0
10
20
30
40
50
60
70

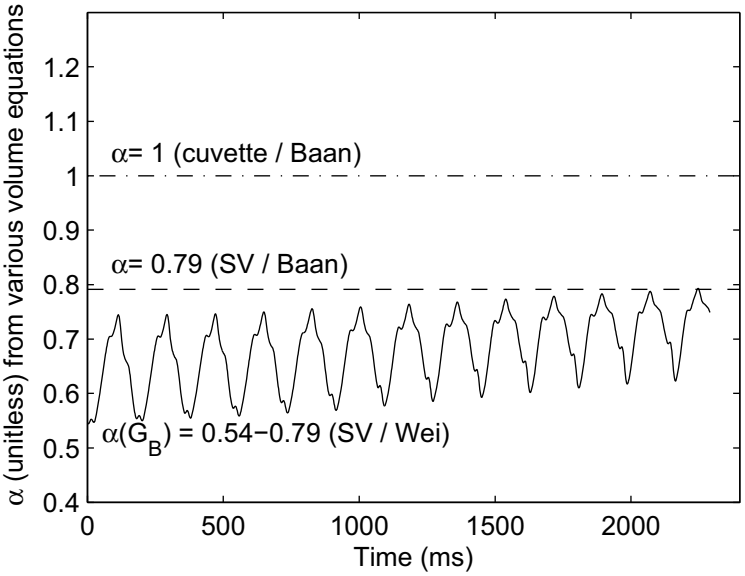
α (unitless) from various volume equations
1.2
1.1
1
0.9
0.8
0.7
0.6
0.5
0.4
α= 1 (cuvette / Baan)
α= 0.79 (SV / Baan)
α(G_B) = 0.54−0.79 (SV / Wei)
0
500
1000
1500
2000
Time (ms)

Mouse No.	Catheter Position*	
	Wall	Center
1	55%	20%
2	80%	21%
3	39%	16%
4	78%	3%
5	36%	0%
6	47%	23%
7	31%	18%
8	62%	9%
mean	53 ± 19%	14 ± 9%